Molecular Forces Caused by the Confinement of Thermal Noise

Mihai D. Morariu, Erik Schäffer,* and Ullrich Steiner†

Department of Polymer Chemistry and Materials Science Center, University of Groningen, Nijenborgh 4, NL-9747 AG Groningen, The Netherlands

(Received 7 November 2003; published 16 April 2004)

We have investigated spontaneous surface instabilities of very thin polymer films. Film stability and the wavelength of the dominating unstable mode were found to depend sensitively on the media adjacent to the film. Our experimental results cannot be explained by van der Waals interactions alone. To account for the presence of an additional destabilizing force, we propose that the geometrical confinement of thermally excited acoustic waves gives rise to a force that is strong enough to destabilize thin films. This thermoacoustic effect is of similar magnitude as van der Waals forces.

DOI: 10.1103/PhysRevLett.92.156102 PACS numbers: 68.15.+e, 05.40.–a, 47.20.Ma, 47.54.+r

Spontaneously amplified capillary waves of a liquid surface reflect the presence of a destabilizing force. The observation of thin film instabilities therefore is a convenient way to quantitatively measure these forces [1]. While the interest in liquid dewetting stems mainly from its technological importance, capillary film instabilities have recently been used to study the role of interfacial forces in the film breakup [1]. Such forces couple to capillary wave spectrum at the liquid surface. The competition of a destabilizing force with the restoring surface tension γ causes the amplification of a narrow band of capillary waves. Examples of destabilizing forces in thin films include van der Waals [1], electrostatic forces [2], or temperature gradients [3].

Additional forces can arise from the spatial confinement of a fluctuation spectrum. One example is the "Casimir effect," an attractive force between two metal plates arising from the confinement of electromagnetic zero-point fluctuations at small plate spacings [4]. Generalized to arbitrary materials in the gap and the adjacent media, this leads to the theory of van der Waals forces [5]. Although the Casimir effect and van der Waals forces are rooted in the quantum theory of electrodynamics, there are analogous effects in classical physics. Forces that arise from the confinement of a fluctuation spectrum were observed in stacks of membranes, liquid crystals, demixing polymer blends, etc. [6]. At sufficiently high temperatures, there should be a similar, but more fundamental, effect caused by thermally excited acoustic fluctuations [5,7,8].

Here we present an experimental study on the destabilization of very thin polymer films. By carefully excluding all known externally applied sources of instabilities, the stability of thin liquid films should be determined exclusively by the van der Waals interactions. Our experiments show, however, the presence of an additional surface field that enhances the film destabilization. We propose that this force arises from the confinement of thermal modes inside the films. Similar to van der Waals forces, this thermoacoustic force is a fundamental effect that needs to be taken into account when glass-forming liquids (such as macromolecules) are confined.

The experimental system consisted of thin polymer films on various substrates. The polymers were polystyrene (PS) ($M_w = 1.92$ kg/mol, $M_w/M_n = 1.06$, $n_f = 1.59$), polymethylmethacrylate (PMMA) ($M_w = 2.50$ kg/mol, $M_w/M_n = 1.07$, $n_f = 1.49$), and polyacrylamide (PAAM) ($M_w = 1.52$ kg/mol, $M_w/M_n = 1.12$, $n_f = 1.45$). PMMA films were spin cast from toluene onto Si, SiO_x, and glass substrates. PS films were spin cast from cyclohexane onto the PMMA substrates and PMMA films were cast from acetic acid onto PS substrates. The PMMA films were dried in vacuum at 80 °C for 5 min prior to annealing. PAAM films were spin cast from water onto SiO_x and dried in vacuum at 100 °C for 4 days.

The substrates were silicon wafers, glass slides, and thick layers of silicon oxide (SiO_x), PS, and PMMA. Silicon wafers (110, B doped) were cleaned in a jet of CO_2 crystals (snow jet), in a "piranha solution" (70% H_2SO_4, 30% H_2O_2) at 80 °C, and then washed in Millipore water. As obtained, the wafers were covered by a 1.6 nm thick SiO_x layer. The refractive index of SiO_x and Si were 1.46 and 4.11, respectively. The glass substrates had refractive indices ranging from 1.5 to 1.7. They were cleaned by snow jet, sonication in ethanol, acetone, and Millipore water for 10 min each and by a chemical etch in a piranha solution. Before use, the substrates were washed in Millipore water and cleaned by snow jet. SiO_x substrates were thermally grown by placing Si wafers into an air-filled oven set to 900 °C for 3.5 h. This resulted in a 110 nm thick SiO_x layer on Si. Before use, the SiO_x substrates were cleaned in the same way as the Si wafers. The refractive index of SiO_x was 1.48. PMMA substrates ($n_s = 1.49$, molecular weight $M_w = 1080$ kg/mol, polydispersity $M_w/M_n = 1.16$) and PS substrates ($n_s = 1.59$, $M_w = 2057$ kg/mol, $M_w/M_n = 1.14$) were made by spin coating from toluene onto Si wafers and dried for 10 min in vacuum at 80 °C. The PMMA layer thickness was 78 nm; the PS layer thickness was 98 nm.

All refractive indices and substrate layer and film thicknesses were measured by imaging ellipsometry (Nanofilm EP3, wavelength 532 nm). After annealing, all samples were imaged by optical microscopy and atomic force microscopy (AFM).

The result of a typical experiment is shown in Fig. 1. A 2.4 nm thick PS film on an oxide covered Si wafer developed a wave pattern after heating above the glass transition temperature of PS [Fig. 1(a)]. The surface pattern was characterized by a single instability wavelength λ obtained by the Fourier analysis shown in Fig. 1(b). An increase in the film thickness by only ≈ 1 nm caused a fundamental change in the film morphology. The defects in Fig. 1(c) reflect the film breakup by heterogeneous nucleation of individual holes [9], a signature that the film is stable with respect to capillary waves.

The film instability in Fig. 1(a) can be analyzed by considering the balance between a destabilizing pressure p and the restoring surface tension γ. This leads to the stability equation for the most unstable wavelength λ [10,11]

$$\lambda = 2\pi\left(-\frac{1}{2\gamma}\frac{\partial p}{\partial \ell}\right)^{-1/2}, \tag{1}$$

where ℓ is the thickness of the liquid film. The sign of the pressure gradient determines the stability condition: a negative pressure gradient destabilizes the film, while layers with a positive value of $\partial p/\partial \ell$ are stable with respect to capillary fluctuations.

In the absence of externally imposed potentials, p arises from the van der Waals potential. For sufficiently small values of ℓ,

$$p_{\mathrm{vdW}} = \frac{A}{6\pi\ell^3}. \tag{2}$$

The Hamaker constant A can assume positive and negative values, corresponding to a destabilizing and stabilizing effect of p_{vdW}. A is approximated by [12]

$$A \approx \frac{3}{4}kT\left(\frac{\varepsilon_s - \varepsilon_f}{\varepsilon_s + \varepsilon_f}\right)\left(\frac{\varepsilon_a - \varepsilon_f}{\varepsilon_a + \varepsilon_f}\right) + \frac{3h\nu_e}{8\sqrt{2}}\frac{(n_s^2 - n_f^2)(n_a^2 - n_f^2)}{\sqrt{n_s^2 + n_f^2}\sqrt{n_a^2 + n_f^2}\left(\sqrt{n_s^2 + n_f^2} + \sqrt{n_a^2 + n_f^2}\right)}, \tag{3}$$

with the dielectric constants ε_i and refractive indices n_i of the three media, and $h\nu_e$ the energy corresponding to the main electronic UV absorption frequency $\nu_e \approx 3 \times 10^{15}$ Hz. The indices correspond to air, film, and substrate, respectively. Note that the first term of the equation accounts for $\approx 10\%$ of the value of A. The error margins of A in Eq. (4) are $\approx 10\%$, compared to more accurate calculations [12].

In analogy to the van der Waals forces, which arise from the confinement of electromagnetic modes, forces stemming from the confinement of thermal noise were also predicted [5,7,8]. The significance of these predictions is somewhat controversial, due to the finite compressibility of liquids at high acoustic frequencies [13]. Polymer melts are, however, highly incompressible. As a consequence, acoustic modes with nanometer wavelengths have a mean free path length of several micrometers [14] and therefore exhibit the necessary coherence to exhibit a Casimir type of confinement pressure in thin films. The predicted acoustic pressure contribution stemming from the confinement of thermal fluctuations in thin supported polymer films is [8]

$$p_{\mathrm{ac}} = \frac{\pi kT}{18\ell^3}. \tag{4}$$

Because A in Eq. (2) is on the order of the thermal energy kT at ambient temperatures for the systems studied here, the destabilizing effect of p_{ac} is comparable to p_{vdW}. In this case, the pressure in Eq. (1) has to be identified with $p = p_{\mathrm{vdW}} + p_{\mathrm{ac}}$.

Since both p_{vdW} and p_{ac} have the same variation with film thickness ℓ, it is a challenge to experimentally distinguish these two effects [15]. Therefore, three independent approaches were employed: (i) the investigation of

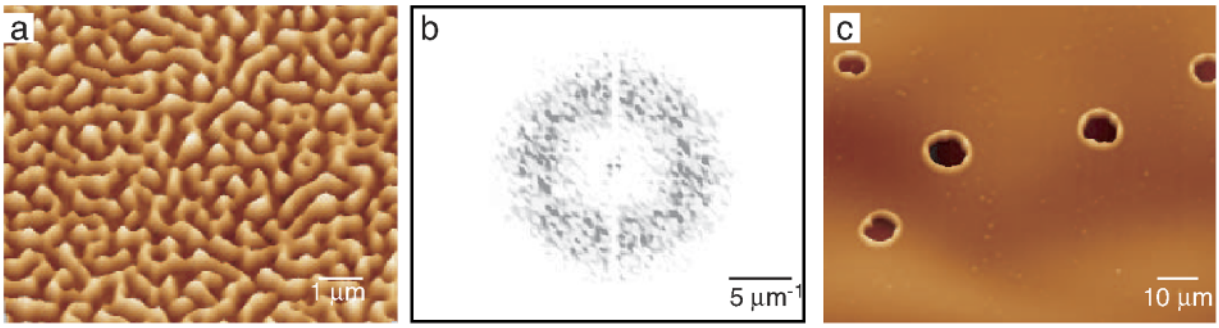

FIG. 1 (color online). Atomic force microscopy (AFM) images of thin polymer films. (a) Capillary instability of a 2.4 nm thick PS film on an oxide covered Si wafer (inset of Fig. 2) (15 min at 50 °C). (b) Fourier transform of (a): $\lambda = 450 \pm 154$ nm. (c) A $\ell = 3.7$ nm thick film is stable for many hours at 50 °C, but forms holes when raising the temperature to 170 °C.

the differing temperature dependence of Eqs. (2) and (4), (ii) the case of opposing pressures p_{vdW} and p_{ac}, and (iii) the dependence of the film instability on the acoustic boundary conditions.

In the first class of experiments, we utilize that p_{ac} varies linearly with T, while A has only a weak temperature dependence determined by the weak variation of n_i and ε_i with T [16]. Films of PS on silicon wafers that were covered by a 1.6 nm thick oxide layer were liquefied by heating. Since the oxide layer has a destabilizing effect on the PS film (which is stable on a pure Si substrate), this setup is particularly sensitive for the detection of p: only films below a critical thickness $\ell < \ell_c$ are unstable [Fig. 1(a)], with a sharp divergence $\lambda \to \infty$ at ℓ_c, where $p = 0$ [1,8].

The results of these experiments are shown in Fig. 2, where the instability wavelength λ extracted from images similar to Fig. 1(a) is plotted versus ℓ. Despite the scatter in the data, changing the annealing temperature from $T = 50\,^{\circ}\mathrm{C}$ to $T = 170\,^{\circ}\mathrm{C}$ clearly causes a shift in the experimentally determined values of the divergence from $\ell_c = 2.4 \pm 0.2$ nm to $\ell_c = 3.0 \pm 0.2$ nm. This enhancement of the film instability caused by the increase in annealing temperature cannot be explained by the (marginal) temperature dependence of A alone (dashed lines in Fig. 2). The incorporation of the temperature dependence of p_{ac} is essential to account for the data.

In the second approach, we chose a system in which p_{vdW} and p_{ac} have opposing signs. While the accurate prediction of A is difficult, its sign can be reliably predicted [12]. A is positive (destabilizing) if the refractive indices of the two media bounding the film [air (n_a), substrate (n_s)] are lower compared to the film (n_f), and negative (stabilizing) if $n_s > n_f > n_a$. From an electromagnetic point of view, polymer films on high refractive index materials are therefore expected to be stable. To demonstrate the effect of the acoustic Casimir pressure, we chose two experimental systems with $n_s \gtrsim n_f$. In such a case, there is a competition between p_{vdW} and p_{ac}. The two experimental systems investigated were PMMA ($n_f = 1.49$) on glass ($n_s = 1.52$) and PAAM ($n_f = 1.45$) on thermally grown SiO_x ($n_s = 1.48$). In both cases, the calculated $p_{vdW} < 0$ with $|p_{ac}/p_{vdW}| \approx 3$ and $|p_{ac}/p_{vdW}| \approx 7$ for PMMA and PAAM, respectively.

Both samples series show the distinct signature of a capillary instability for film thicknesses smaller than 12 nm (insets of Fig. 3). As van der Waals forces alone are stabilizing for both films, the observation of a capillary instability is direct evidence for the presence of a destabilizing force. Figure 3 shows the variation of λ versus ℓ for PMMA and PAAM films, respectively. The data are in reasonable agreement with the predictions from Eq. (1) using $p = p_{vdW} + p_{ac}$.

For PMMA on glass, we have repeated the experiment from Fig. 3(a) for substrates with $n_s = 1.51$ and $n_s = 1.61$, finding unstable PMMA films. On glass substrates with $n_s = 1.71$, on the other hand, capillary instabilities were not observed, corresponding to the dominance of the stabilizing van der Waals pressure $|p_{vdw}| > p_{ac}$.

A third experimental test involves the variation of the acoustic boundary conditions. A prerequisite for the confinement of long wavelength thermal modes is the acoustic isolation of the film from the surrounding media, implying a large enough difference in densities and elastic properties of the film and the substrate [8]. While this is the case for polymers on glass and silicon, we expect the suppression of p_{ac} on substrates that have similar acoustic properties as the films. To this end, two comparative studies were made: (i) PS on SiO_x ($n_s = 1.48$) compared to PS on PMMA ($n_s = 1.49$) and (ii) PMMA on glass with $n_s = 1.61$ compared to PMMA on PS ($n_s = 1.59$). In both cases, the optical properties of the two

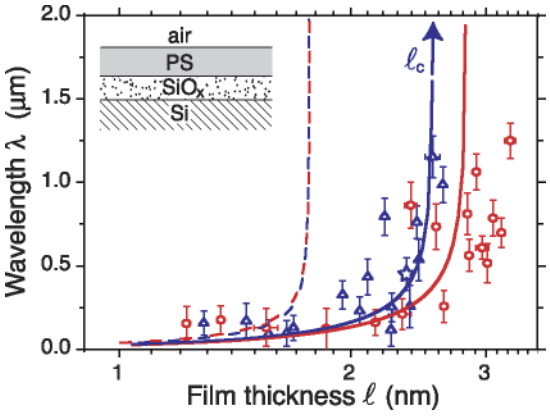

FIG. 2 (color online). Temperature dependence of the capillary instability. PS films on Si wafers covered by a 1.6 nm thick SiO_x layer (inset) show a capillary instability for $\ell < \ell_c$. The plot of λ vs ℓ shows a temperature increase of the experimentally determined cutoff from $\ell_c = 2.4 \pm 0.2$ nm at $T = 50\,^{\circ}\mathrm{C}$ to $\ell_c = 3.0 \pm 0.2$ nm at $T = 170\,^{\circ}\mathrm{C}$. The lines are predictions of Eq. (1) with $p = p_{vdW} + p_{ac}$ (dashed lines: $p_{ac} = 0$). The star corresponds to Fig. 1(a).

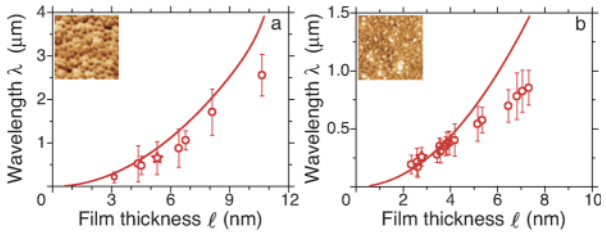

FIG. 3 (color online). Capillary instability of films with stabilizing van der Waals forces. Since $n_f < n_s$, (a) PMMA on glass ($T = 130\,^{\circ}\mathrm{C}$) and (b) PAAM on SiO_x ($T = 170\,^{\circ}\mathrm{C}$) are expected to be stable when only van der Waals forces are considered ($p_{ac} = 0$), but experiments show capillary instabilities [insets: $5 \times 5\ \mu m^2$ AFM images corresponding to the data points marked by stars]. The lines are predictions from Eq. (1) with $p = p_{vdW} + p_{ac}$.

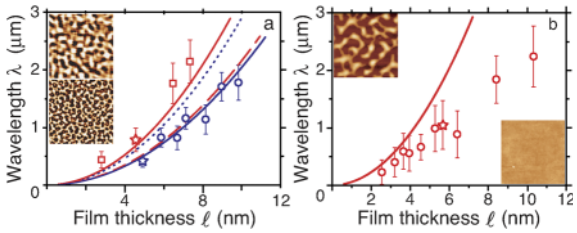

FIG. 4 (color online). Dependence of the film instability on the acoustic boundary condition. (a) Comparison of PS on PMMA (□) and PS on SiO_x (○). The lack of acoustic confinement for PS on PMMA [solid line: $p_{ac} = 0$; dashed line: p_{ac} from Eq. (4)] gives rise to larger values of λ compared to PS on SiO_x [solid line: p_{ac} from Eq. (4); dotted line: $p_{ac} = 0$). (b) PMMA on glass ($n_s = 1.61$) (○, top-left inset) compared to PMMA on PS (bottom-right inset). Since $p_{vdW} < 0$ (stabilizing), only PMMA on glass with $p = p_{vdW} + p_{ac} > 0$ (solid line) is unstable. The insets show typical $5 \times 5\ \mu m^2$ AFM images corresponding to the data points marked by the stars.

substrate types are similar, implying comparable values of p_{vdW}. Differences in the observed film instability should therefore be due to differing values in p_{ac}.

Figure 4(a) shows the comparison of PS on SiO_x and PMMA substrates. A visual comparison of the instability of ≈ 4.7 nm thick PS films on the two substrates (inset) reveal a large difference in λ, indicative for a difference in destabilizing pressures. The quantitative analysis reveals systematically lower values of λ for PS on SiO_x, compared to PS on PMMA. This difference is readily explained by the lack of confinement of acoustic modes ($p_{ac} \approx 0$) for PS on PMMA (and therefore a contribution of p_{vdW} alone), compared to PS on SiO_x, where the sum of p_{vdW} and p_{ac} gives rise to the lower values of λ.

The complementary experiment is the investigation of PMMA films on high refractive index glass ($n_s = 1.61$) and on PS ($n_s = 1.59$) substrates [Fig. 4(b)]. In this case, we find results that reflect the competition of p_{vdW} and p_{ac} discussed above (Fig. 3). Since the substrates have higher refractive indices than PMMA, p_{vdW} exerts a stabilizing pressure on the films. In the case of the PS substrate (where $p_{ac} \approx 0$) the PMMA films are therefore stable and do not exhibit a capillary instability (bottom-right inset). On the glass substrate, on the other hand, the dominating effect of the acoustic disjoining pressure ($p_{ac} > |p_{vdW}|$) causes a spontaneous film instability (top-left inset) predicted by Eq. (1).

Residual potentials or stresses in the film are other sources of instabilities [17] . We took utmost care to eliminate or minimize such additional effects [18].

Our study demonstrates the high sensitivity of film instabilities to forces acting over small distances. The complementary nature of the three experimental approaches allows us to identify forces caused by the confinement of thermal noise, confirming all predictions [15] concerning the acoustic Casimir effect.

This work was partially funded by the "Stichting voor Fundamenteel Onderzoek der Materie" (FOM) and the Dutch Polymer Institute (DPI).

*Max Planck Institute of Molecular Cell Biology and Genetics, Pfotenhauerstrasse 108, D-01307 Dresden, Germany.
†Electronic address: u.steiner@chem.rug.nl

[1] R. Seemann, S. Herminghaus, and K. Jacobs, Phys. Rev. Lett. **86**, 5534 (2001).
[2] E. Schäffer, T. Thurn-Albrecht, T. P. Russell, and U. Steiner, Nature (London) **403**, 874 (2000).
[3] E. Schäffer, S. Harkema, R. Blossey, and U. Steiner, Europhys. Lett. **60**, 255 (2002).
[4] H. B. G. Casimir, Proc. K. Ned. Akad. Wet. **B51**, 793 (1948).
[5] I. E. Dzyaloshinskii, E. M. Lifshitz, and L. P. Pitaevskii, Adv. Phys. **10**, 165 (1961).
[6] M. Kadar and R. Golestanian, Rev. Mod. Phys. **71**, 1233 (1999).
[7] O. Bschorr, J. Acoust. Soc. Am. **106**, 3730 (1999).
[8] E. Schäffer and U. Steiner, Eur. Phys. J. E **8**, 347 (2002).
[9] K. Jacobs, S. Herminghaus, and K. R. Mecke, Langmuir **14**, 965 (1998).
[10] A. Vrij, Discuss. Faraday Soc. **42**, 23 (1966).
[11] F. Brochard Wyart and J. Daillant, Can. J. Phys. **68**, 1084 (1990).
[12] J. N. Israelachvili, *Intermolecular and Surface Forces* (Academic, London, 1991).
[13] D. Y. C. Chan and L. R. White, Physica (Amsterdam) **122A**, 505 (1983).
[14] C. J. Morath and H. J. Maris, Phys. Rev. B **54**, 203 (1996).
[15] M. D. Morariu, E. Schäffer, and U. Steiner, Eur. Phys. J. E **12**, 375 (2003).
[16] The reduction of γ with increasing temperature in Eq. (1) changes the shape of the dashed lines in Fig. 2, but not their value of ℓ_c. The temperature variations of A and γ were taken into account in all calculations.
[17] Eur. Phys. J. E **12**, 359 (2003).
[18] Some of the data in Figs. 2–4 lie below the predicted values. This could arise from the simplifying assumptions made in the derivation of Eq. (4) (for details, see Ref. [8]) or from small additional potentials arising, for example, from static charges at the polymer surface or small temperature gradients.